33rd Annual International Conference of the IEEE EMBS
Boston, Massachusetts USA, August 30 - September 3, 2011

Model-based 3D/2D Deformable Registration of MR Images

Bahram Marami, Shahin Sirouspour and David W. Capson

Abstract— **A method is proposed for automatic registration of 3D preoperative magnetic resonance images of deformable tissue to a sequence of its 2D intraoperative images. The algorithm employs a dynamic continuum mechanics model of the deformation and similarity (distance) measures such as correlation ratio, mutual information or sum of squared differences for registration. The registration is solely based on information present in the 3D preoperative and 2D intraoperative images and does not require fiducial markers, feature extraction or image segmentation. Results of experiments with a biopsy training breast phantom show that the proposed method can perform well in the presence of large deformations. This is particularly useful for clinical applications such as MR-based breast biopsy where large tissue deformations occur.**

I. INTRODUCTION

Volumetric magnetic resonance (MR) and computed tomography (CT) images provide detailed anatomical information for medical diagnosis and intervention. Surgical plans based on pre-operative images often have to be updated using information obtained from interventional imagers to compensate for possible movement and deformation of the underlying soft tissue. Long acquisition times restrict the amount of data that can be collected intraoperatively. For example, real-time MR imaging is only feasible when the volume of the scan and image resolution are reduced. Consequently, intraoperative images lack the detailed and comprehensive information that is available in high-resolution preoperative 3D images. Furthermore, interventional MR and ultrasound (US) images have lower signal-to-noise ratio than that of diagnostic MR images [1].

Preoperative and intraoperative images can be fused in a registration process to produce detailed up-to-date volumetric data about the patient anatomy. Nonrigid registration algorithms should be employed in medical applications involving soft-tissue deformation, e.g. in breast imaging and biopsy procedures. It should be noted that image registration is an ill-posed problem by itself [2]. In addition, nonrigidity of 3D/2D registration makes the problem ill-conditioned and nonlinear. Therefore, the registration problem should be regularized for a solution to exist.

Physics-based models associating geometry, dynamics and material properties of the object can be used as a regularizer in image registration. In breast imaging, finite-element (FE) based continuum mechanics models have been used to predict mechanical deformation during MR-guided biopsy [3], and to validate nonrigid registration algorithms [4]. Moreover, they have been employed to model multi-object deformations in the abdominal region for deformable image registration [5]. The similarities (or differences) between the two images are used to deform the FE model in nonrigid registration. In most cases, local image information such as surfaces and extracted feature points are employed in the calculation of external and internal forces applied to the discretized FE mesh [6], [7]. In [3], the movement of the breast tissue was tracked using landmarks tapped to its surface.

The above methods are all concerned with 3D/3D or 2D/2D registration. They require various user interventions such as affixing fiducial markers, extracting image features and constructing surface models. In this paper, we propose a FE model based method for deformable registration of preoperative 3D to a sequence of intraoperative 2D MR images. A dynamic linear elastic deformation model imposes a regularization constraint on permissible volume transformations based on an image similarity criterion. The model allows us to incorporate the dynamic behavior of tissue deformation into the registration process; it establishes physically meaningful temporal and spatial correlations among the 2D images taken at successive sample times from different cross-sections of the tissue. The model and image information are fused through a filtering process that iteratively estimates the deformation of the 3D volumetric image. The observation error for the filter can be produced based on sum of squared differences (SSD), correlation ratio (CR), or mutual information (MI) between corresponding 2D image slices.

II. METHODS

A. Static Model

Image registration involves finding a displacement field u such that a transformed template image $T[u]$ becomes "similar" to a reference image R. The objective function to be minimized is [2]:

$$J(u) = D(T[u], R) + \alpha S(u); \quad \alpha \in \Re_+ \tag{1}$$

where D is a distance measure between two images and S is a regularization term that would ensure the resulting displacement field is "reasonable". A similarity measure with a negative sign could also be used instead of the distance measure. The linear elastic energy of the deformable body is used as the regularization term in this paper where α weights its relative importance compared with the distance measure. The deformation model is discretized using FEM in the spatial domain with a volumetric tetrahedral mesh. The

B. Marami, S. Sirouspour and D. W. Capson are with the Department of Electrical and Computer Engineering, McMaster University, Hamilton, Ontario L8S 4K1, Canada maramib@mcmaster.ca, sirouspour@ece.mcmaster.ca, capson@mcmaster.ca

linear elastic energy for the discretized model in (1) can be written as [6]:

$$S(u) = \frac{1}{2} u^T K u \tag{2}$$

where K is the global stiffness matrix associated with the volumetric mesh, and u is the vector of nodal displacements. The displacement of any point of the image volume can be computed using the shape function of the element containing the point as follows

$$u_{in}(x) = \sum_{i=1}^{4} N_i^{el}(x) u_i^{el}(x) \tag{3}$$

where $u_{in}(x)$ is the displacement for the internal point and $u_i^{el}(x)$ is the displacement of the vertex points of the element. $N_i^{el}(x)$ is the linear shape function of the elements given in [8]. If J in (1) has a minimum at u, its first derivative must vanish, *i.e.*

$$\frac{\partial J(u)}{\partial u} = \frac{\partial D(T[u], R)}{\partial u} + \alpha K u = 0 \tag{4}$$

which can be rewritten as the following set of nonlinear equations

$$K u = f(u) = -\frac{1}{\alpha} \frac{\partial D(T[u], R)}{\partial u} \tag{5}$$

Here $f(u)$ is the vector of nodal forces applied to the mesh. The solution to (5) is the displacement field corresponding to the minimum of (1).

B. Dynamic Model

The force vector $f(u)$ in (5) is a nonlinear function of the displacement field u. An iterative numerical method has to be employed to solve the nonlinear system of equations in (5). To this end, we consider the following second-order dynamic model for the motion of deformable objects [8]:

$$M\ddot{u} + C\dot{u} + Ku = f(u) \tag{6}$$

Here M is the mass matrix of the elements concentrated at nodes, and $C = \beta M + \gamma K$ is the damping matrix for constant values of β and γ. It is noted that the steady-state equilibrium of this dynamic system is the solution to the static system of equations in (5). In (6), the dynamic forces $M\ddot{u}$ and $C\dot{u}$ tend to smoothly drive the system towards this equilibrium. The dynamic equations can be solved using existing implicit or explicit numerical integration routines over time. A dynamic model also allows for real-time intraoperative registration of a dynamically changing organ. It provides a temporal correlation model for the images taken at different sample times. Such situations can arise, for example, in real-time MR based biopsy interventions where the soft tissue undergoes deformation due to the force of needle insertion. Therefore, our proposed method can be used in such circumstances for dynamic image registration.

The solution for (6) can be obtained more effectively by using the transformation $u = \phi v$ on the n finite element nodal point displacements, where columns of ϕ are eigenvectors of $M^{-1}K$ [8]. With this change of variables, (6) can be written as:

$$\hat{M}\ddot{v} + \hat{C}\dot{v} + \hat{K}v = \hat{f} \tag{7}$$

where $\hat{M} = \phi^T M \phi$, $\hat{C} = \phi^T C \phi$, $\hat{K} = \phi^T K \phi$ are diagonal matrices, and $\hat{f} = \phi^T f$. Assuming that $M^{-1}K$ is full rank, the equilibrium equations become decoupled. The fast modes of (7) can be eliminated without affecting the steady-state solution, resulting in a significant reduction in the computation time.

C. 3D/2D registration

Starting with an undeformed mesh, the deformation field has to be continuously updated based on the dynamic model in (7) and information from the 3D preoperative (undeformed) volume and the 2D slices of intraoperative (deformed) images. In an optimization paradigm, each iteration would take the solution one step closer to the minimum of the objective function (1). For example in a gradient-decent search, the steps are proportional to the negative of the gradient of the objective function at the current state. In our algorithm, the "distance" between the current intraoperative 2D image and the corresponding slice of the 3D image is the observation error in a Kalman-type filtering process for the estimation of the mesh deformation.

For each 2D intraoperative image, the corresponding 2D slice of the preoperative image is found based on the position and the orientation of a virtual 2D interventional MR plane. For any point y in the domain of reference (intraoperative) image, its displacement in the template domain is computed as:

$$dy = -\lambda \nabla D(T[u(y)], R); \quad \lambda \in \Re_+ \tag{8}$$

where R is the 2D reference (intraoperative) image and $T[u(y)]$ is the 2D template image interpolated from the preoperative volume in each step. An analytical approach is proposed in [9] to compute the derivative of three different distance (similarity) measures. By letting h denote a generic intensity comparison function, (8) can be written as:

$$dy = -\lambda h(T[u(y)], R) \nabla T[u(y)] \tag{9}$$

where $\nabla T[u(y)]$ is the gradient of the template image at y in every iteration. The definitions of three distance (similarity) measures SSD, CR and MI, and the corresponding intensity comparison functions are given in [9]. It should be noted that dy is a 3×1 vector and is not restricted to the plane of the 2D images.

The displacement of regular grid points of the 2D slice are the observation errors in the filtering process and can be related to the nodal displacements (system states) using elemental shape functions. The discretized dynamic deformation model (6) and observation equations can be written in the following general form:

$$\begin{aligned} v(k+1) &= Av(k) + B\hat{f} \\ z(k) &= Hv(k) \end{aligned} \tag{10}$$

Here v and z are state and observation vectors, and A, B, and H are the state transition matrix, the model input matrix and the model output matrix, respectively. Note that H contains both the transformation matrix ϕ and the linear shape function of the tetrahedral elements.

The system states, which include the deformation of the 3D mesh, are estimated using a Kalman-like filter at each time step. The filter equations can be found in [10]. In (10), $\hat{f}$ is modeled as white Gaussian noise with probability distribution of $p() = N(0, S)$. Each iteration of the registration algorithm involves the following steps:

1) For each 2D reference plane from the intraoperative volume, find the corresponding 2D template plane from the intraoperative volume.

2) Using (9), find the displacement field for the regular grid points of the 2D template plane.

3) Update the state estimates based on the observation prediction error $z_k - H\hat{v}_k^-$ using $\hat{v}_k = \hat{v}_k^- + K_k(z_k - H\hat{v}_k^-)$. Here $\hat{v}_k^-$ is the vector of state estimates from the pervious step and K_k is the filter gain. The displacement of FE mesh vertices points can then be updated using $u = \phi v$.

In case of registering a static deformed tissue, the 3D estimation will eventually converge to a steady-state solution. In a dynamic case where the object deformation varies over time, the estimated 3D deformation at each step represents the object state at the corresponding time.

III. EXPERIMENTS AND RESULTS

A triple modality biopsy training breast phantom (CIRS model 051) is used for obtaining the experimental data. Two 3D volumes of high-resolution (512×512×136) MR images have been taken from the undeformed and deformed phantom using a GE 3T Signa MRI machine. This is essentially a static deformable registration problem. The apparatus developed for deforming the phantom during imaging is shown in Fig. 1 (a). This structure is made using plexiglass and is MR compatible. There are two stabilizing plates between which can compress the phantom. Four pairs of screws and nuts which are connected to the plates are used to adjust the distance between them to deform the phantom. Moreover, four capsules of vitamin E are placed on the framework as landmarks to match the coordinates of the deformed and undeformed image data after taking images. In Fig. 1 (b), an x-y view of the undeformed (top) and deformed (bottom) image data are also shown.

A cubic mesh of tetrahedral elements which contains the whole volume of the deformed and undeformed data is created using the COMSOL Multiphysics and Simulation Software. In Fig. 2, the volumetric mesh used for registration is depicted before (a) and after (b) deformation with two 2D planes across the mesh. The mesh has 15112 elements and 3067 nodal points. Young's elasticity modulus E and Poisson's ratio ν which characterize an isotropic linear elastic material [8] are chosen as 10^5 and 0.45, respectively. Since the model is essentially used to regulate the registration process, its geometrical or material accuracy is not critical for the success of the approach. The model parameters can

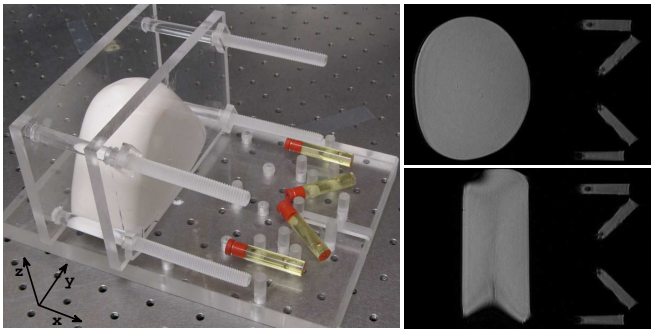

(a) (b)

Fig. 1. (a) the apparatus, (b) x-y views of undeformed (top) and deformed (bottom) images

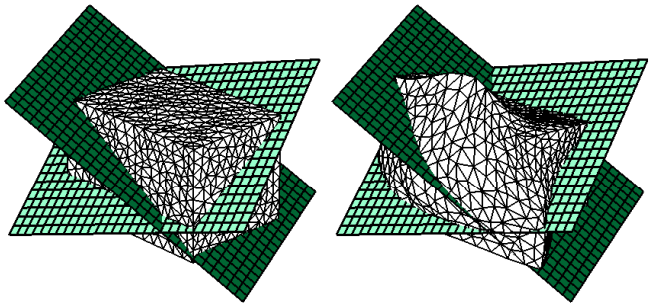

(a) (b)

Fig. 2. (a) undeformed, (b) deformed FE mesh with 2D planes across them

be tuned to obtain a desirable outcome. The two 2D planes across the FE mesh are demonstrating two different 2D interventional MR planes (reference) (a) and the corresponding 2D planes in the preoperative data set (template) (b).

As can be seen from Fig. 1(b), the phantom undergoes both translation and deformation for which the registration algorithm has to account. In Fig. 3, the registration results utilizing a sequence of 15 2D intraoperative planes are shown. All these planes pass through the center point of the data volume and the normal vector to the plane is $\vec{n} = [0 \quad cos(\theta) \quad sin(\theta)]^T$ where $0 \leq \theta < 180°$. Registration of the template images (left column) to references images (middle column) produces deformed template images (right column) which are very similar to the reference images. Here the registration is performed based on SSD and other measures are computed for the region of interest in each iteration. In Fig. 4(a), the evolution of similarity (distance) measures between 3D volumes of pre- and intraoperative data during the iterative registration process are shown. The change of similarity (distance) measures between the 2D reference and template images are also displayed in Fig. 4(b). It can be seen that for every fixed 2D reference plane, the model is updated in 15 iterations.

A quantitative comparison of the three distance (similarity) measures for registration performed based on each of these measures is given in Table 1. The gray scale values for the experimental images are between 0 and 255. For a better comparison, normalized mutual information (NMI) is computed instead of MI because $0 \leq$NMI≤ 2 for any two sets of image data. Also the value of SSD is divided by the

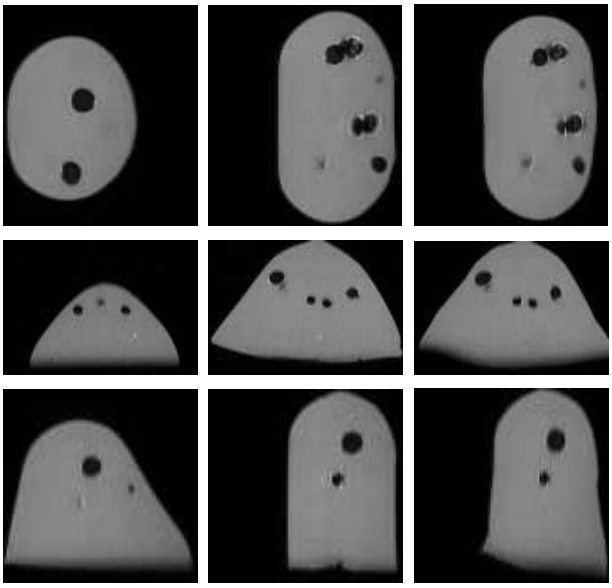

Fig. 3. Top to bottom: x-y, y-z, and x-z views; left to right: preoperative (template), intraoperative (reference), and registered (deformed template) images

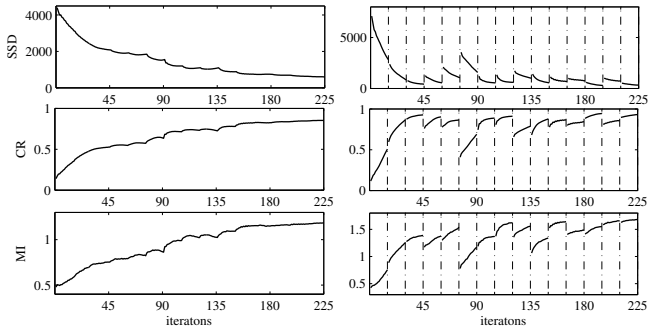

(a) (b)

Fig. 4. The evolution of distance and similarity measures throughout the registration process (a) 3D volumes, (b) sequences of 2D slices. A total number of 15 2D slices have been used for each of which the model is updated in 15 iterations

number of voxel points. The perfect match happens when SSD is close to zero, CR is close to 1 and NMI is close to 2. It can be concluded from Table 1 that SSD-based registration outperforms both CR and MI-based registration methods. The registration algorithm works well with the SSD measure since the images are from a single modality. MI is generally an effective similarity measure for 3D multi-modality registration. However, in our case of 3D/2D registration, a relatively small number of pixels is available to form histogram. The resulting sparse joint histogram is the main reason for the relatively poor performance of the MI-based registration compared to the other measures. Finally, it should be noted that the deformation for the experimental data is static and rather large. The results are expected to further be improved when using the algorithm to dynamically track the deformation of a soft tissue.

TABLE I

REGISTRATION BASED ON DIFFERENT MEASURES

measures	SSD	CR	NMI
SSD-based	290.1	0.938	1.141
CR-based	341.8	0.926	1.123
MI-based	450.3	0.882	0.970

IV. CONCLUSIONS AND FUTURE WORK

A model-based 3D/2D deformable image registration algorithm was proposed in this paper. The registration was carried out within a state estimation framework using a dynamic FE linear elastic deformation model. The state estimates are updated using similarity measures between the intraoperative 2D MR image and the corresponding 2D plane of the preoperative MR volume. The algorithm is only based on pixel and voxel values of pre- and intraoperative images and does not require image segmentation or feature extraction. Experimental results carried out with a breast phantom tissue showed that a 3D volume of preoperative MR images can be effectively registered to a sequence of 2D intraoperative MR images even in the presence of a very large deformation. This makes the algorithm particularly suitable for real-time tracking of tissue deformation using 2D interventional MR images in applications such as breast biopsy.

In the future, the algorithm will be extended to 3D/2D registration of pre-operative MR or CT to intraoperative US images. The proposed algorithm is computationally intensive but the computations are highly parallel in nature. We are currently working on the implementation of the algorithm on a graphics processing unit (GPU) to speed up the registration for real-time applications.

REFERENCES

[1] B. Fei, J.L. Duerk, D.T. Boll, J.S. Lewin and D.L. Wilson, "Slice-to-Volume Registration and its Potential Application to Interventional MRI-Guided Radio-Frequncy Thermal Ablation of Prostate Cancer," *IEEE Trans. on Med. Imaging*, vol. 22(4), 2003, pp. 515-525.

[2] J. Modersitzki, *Numerical Methods for Image Registration*, Oxford, 2004

[3] F.S. Azar, D.N. Metaxas and M.D. Schnall, "A Finite Element Model of the Breast for Predicting Mechanical Deformations During Biopsy Procedures," *IEEE Wsh on Math. Meth. in Biomed. Img. Anal.*, Hilton Head Island, SC , USA, 2000, pp. 38-45.

[4] J.A. Schnabel, C. Tanner, A.D. Castellano-Smith, A. Degenhard and M.O. Leach, "Validation of Nonrigid Image Registration Using Finite-Element Methods: Application to Breast MR Images," *IEEE Trans. on Med. Imaging*, vol. 22(2), 2003, pp. 238-247.

[5] K.K. Brock, M.B. Sharpe, L.A. Dawson, S.M. Kim and D.A. Jaffray, "Accuracy of Finite Element Model-Based Multi-Organ Deformable Image Registration," *Med. Phys.*, vol. 32(6), 2005, pp. 1647-1659.

[6] M. Ferrant, A. Nabavi, B. Macq, F.A. Jolesz, R. Kikinis and S.K. Warfield, "Registration of 3-d Intraoperative MR Images of the Brain Using a Finite-Element Biomechanical Model," *IEEE Trans. on Med. Imaging*, vol. 20(12), 2001, pp. 1384-1397.

[7] A. Nabavi, P.M. Black, D.T. Gering, C.F Westin, V. Mehta, R.S. Pergolizzi, M. Ferrant, S.K. Warfield, N. Hata, R.B. Schwartz, W.M. Wells, R. Kikinis and F.A. Jolesz, "Serial Intraoperative Magnetic Resonance Imaging of Brain Shift," *Neurosurgery*, vol. 48(4), 2001, pp. 787-798.

[8] K.J. Bathe, *Finite Element Procedures*, Englewood Cliffs, NJ, Prentice Hall; 1996.

[9] C. Chefd'Hotel, G. Hermosillo and O. Faugeras, "A Variational Approach to Multi-Modal Image Matching," *IEEE Wsh. on Var. Le. Set Meth.*, Canada, 2001, pp. 21-28.

[10] G. Welch and G. Bishop, "An Introduction to the Kalman Filter," *Uni. of North Carolina*, TR 95-041; 2006.